

*Full length article***GEOCHEMISTRY OF PAB SANDSTONE EXPOSED IN LAKI RANGE LOWER INDUS BASIN: PROVENANCE AND TECTONIC IMPLICATIONS**

G.M. Thebo<sup>1</sup>, M.H. Agheem<sup>1\*</sup>, A.H. Markhand<sup>1</sup>, M.A. Solangi<sup>2</sup>, M.K. Samoon<sup>1</sup>, K.A. Memon<sup>1</sup>, M.A. Jamali<sup>1</sup>

1. Centre for Pure and Applied Geology, University of Sindh, Jamshoro. Pakistan

2. Department of Geology. Mirpurkhas Campus. University of Sindh, Jamshoro. Pakistan

**Abstract**

Geochemistry of the late Cretaceous Pab Sandstone deposited at the Laki Range, Southern Indus basin, was carried out in order to acquire a better knowledge of the source rock and paleoclimate. The unit in the studied region comprise predominantly sandstone, with some mudstone. The major element geochemistry of Pab Sandstone suggests that the samples were composed of abundant SiO<sub>2</sub>, Al<sub>2</sub>O<sub>3</sub>, CaO, and Fe<sub>2</sub>O<sub>3</sub>. Other major oxides comprise less than 2 wt. %. Major element discriminatory diagrams additionally imply that Pab sediments originated from a granitic source. The idea that the Pab sediments were generated by a granitic source is further supported by the rich concentration of trace elements including Zr, La Th, Ba, and Sr, in contrast to V, Ni, Cr, Co, and their ratios. It is conceivable that the Pab Sandstone was formed by sediments from granitic rocks, as indicated by the La/Sc and Th/Co model, as well as the TiO<sub>2</sub> and Zr plots. The measured Plagioclase Index of Alteration (PIA) values, which range from 54.35 to 84.89, and the Chemical Index of Alteration (CIA), which ranges from 53.81 to 79.60, indicate that the studied sediments experienced moderate to strong weathering under warm, humid climate conditions. Geochemical findings indicate that the Pab Sandstone sediments originated from the vast Indian Shield (Craton)

**KEYWORDS:** Pab Sandstone, Laki Range, Indus Basin, XRF, Provenance

\*Corresponding author: (Email: mhagheem@usindh.edu.pk, Phone: 0092-3339401460)

**1. INTRODUCTION**

The term Pab Sandstone was first used by Vredenburg [1] which originated from the Pab Range. [2] designated the area of west of Wirahab Nai, at latitude 25°31'12" N and longitude 67°00'19" E, as the type section for the unit exhibiting a thickness of 490 meters. The Pab Sandstone in the Northern Laki Range is characterized by an exceptionally thick succession of sandstone, with some gravel beds and a relatively low volume of fine lithologies; such as silt and mud. The abundant cross bedding; both planar and trough, is reflected in this lithostratigraphic unit. Compared to planar cross bedding, trough

cross bedding is more prevalent. It is overall red to reddish brown in color and medium to coarse grained in size, with moderate to high compaction. The sandstone and mudstone beds also contain other typical sedimentary structures like asymmetrical ripple marks and mud cracks. The lithologic trend in the gravel beds exhibit a discernible fining up at specific locations within the Pab Sandstone outcrops. The non-clastic sequences of the Fort Munro Formation lie beneath the unit, at few places in the study area whereas in most part of the study area lower contact of the formation is not exposed, while the Khadro Formation lies

on top of it. Maastrichtian age is attributed to the Pab Sandstone strata based on fauna [1, 3]. The provenance analyses are typically performed to identify the source area of the sediment by utilizing different stratum properties. Since different types of source rocks produce different suits of detrital minerals, they can be used to reveal characteristics specific to the source rock from which they originated. The geochemical makeup of siliciclastic rocks is widely utilized to identify their composition, weathering history, and aid in the paleogeographic reconstruction of their original terrains. Additionally, information regarding provenance, tectonics, and paleoclimate can be obtained from their geochemical synthesis [4, 5, 6, 7, 8, 9, 10, 11].

## 2. GEOLOGICAL SETTING

The study area is part of the Laki Range in Southern Indus Basin, Sindh, Pakistan. The Pab Sandstone stratigraphic section exposed in the northern extremities of the Laki Anticline of the Laki Range (Survey of Pakistan Topographic sheet number 35 N/16 that is part of Hunting Survey Corporation geologic map number 11 Bela 35 J-N) is selected for present study. This anticline is part of the Laki Range which in turn is fold and thrust belt, and is oriented in a North – South direction at regional scale. Moreover, this anticline has steep eastern flank and moderately dipping western flank, thus it is asymmetrical in nature. A north-south thrust fault system intersects the steep eastern slope, with potential displacement of up to 1000 meters [17]. The oldest rocks in the base are exposed when this anticline reaches its maximum crest height in the northern extremes of the Laki Range. These rocks are subsequently being worn by ephemeral rivers.

The various localities within the Sulaiman and Kirthar Fold-Thrust belts of the Middle and Lower Indus Basin represent the exposures of the late Cretaceous Pab sandstone. The Middle Indus Basin has been the focus of much research on this significant lithostratigraphic unit, primarily in relation to facies analysis, provenance, and reservoir characteristics [12, 13, 14, 15, 16]. While the studies mentioned above provide a good overview of the deposition, sedimentary source, transportation, and diagenetic character of the Pab Sandstone, further discussion of the geochemistry including major and trace elements of the exposures of this rock unit in the Laki Range, Southern Indus Basin is needed. The current study aims to infer the provenance, tectonics, and paleoclimate utilizing geochemical analysis on a prominent stratigraphic section of the Pab Sandstone, namely the Burr Dhoro (BD) section in the Laki Range (Fig. 1).

The elevation of the Manchhar Formation (Miocene-Pliocene) and recent sediments show that the deformation of this anticline persisted well into the Pleistocene, even after the Miocene [17]. The oldest unit in the region is the Fort Munro Formation, while the youngest unit is the Dada Conglomerate. The region is made up of exposed Cretaceous to Recent sedimentation records. Other than that, the Southern Indus Basin does not have any exposed Cretaceous to Recent age sedimentary strata. The occurrence of many lithologic characteristics in the area suggests that the entire sedimentation stack indicate events of sea level variations. In this location, basaltic flows in Paleocene age strata are also observed [18, 19]. The research area is bordered on the west by the Kirthar Range and Axial Belt, which includes Bela Ophiolites and on the east by the Thar desert and the Nagar Parker igneous complex (Indian shield).

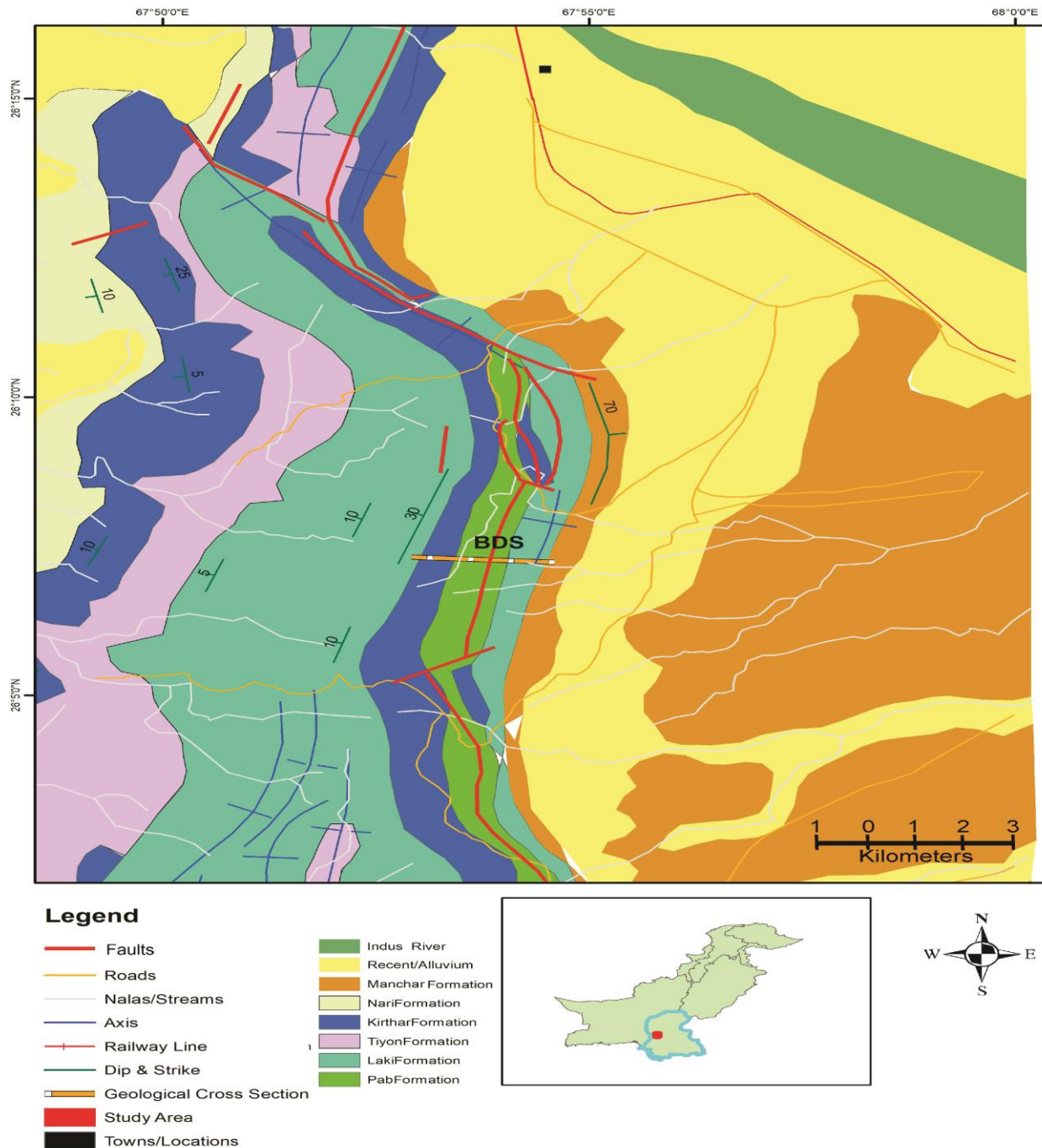


**Fig. 1.** The geological map showing the studied section along with lithologies, in the inset the index map of Pakistan marking the study area

### 3. SAMPLING AND ANALYTICAL METHODS

During field work, the rock samples were taken from the Burr Dhoro (BD) section, with a focus on the Pab strata. From the targeted region, a total of sixteen (16) samples were collected. Particular attention was given to recording every difference in lithology during

the sampling process. Out of all the collected samples, nine (09) representative samples were chosen for the major and trace element geochemistry. Prior to the number these samples were labeled with the prefix BD designating the name of the section sampled. The description of the selected samples is given in Table 1. The S4 Pioneer X-Ray Fluorescence Spectrometer of

the Bruker AXS, Germany, was utilized for the geochemical analyses comprising the major and trace elements for the chosen samples. The XRF apparatus was operated using "Spectra Plus," a common software program that measures the various elements included in the rock samples at various detection limits. Geochemical elemental analyses was performed using the Geo Quant, which is utilized for marketed earth materials. For the rock samples under study, the XRF machine's working parameters were 7 mA of current and 27 kV of voltage. Using the Geomajor application of XRF, the major element oxides ( $\text{SiO}_2$ ,  $\text{Al}_2\text{O}_3$ ,  $\text{TiO}_2$ ,  $\text{Fe}_2\text{O}_3$ ,  $\text{MnO}$ ,  $\text{CaO}$ ,  $\text{MgO}$ ,  $\text{Na}_2\text{O}$ ,  $\text{K}_2\text{O}$ ,  $\text{P}_2\text{O}_5$ ) were determined. For major elements, analytical precision is typically less

than 2% relative. The USGS rock standards were used for the calibration. Major element data was reported using normalized percentages. [20] as well as [21] have evaluated the XRF analytical method in extensive detail. Using pressed powder pellets, the aforementioned X-ray fluorescence spectrometer has also been used to determine trace element concentrations. The best fraction of the chosen samples was meticulously chosen and thoroughly crushed. Additionally, extremely finely powdered samples have been homogenized using the conning and quartering procedure to circumvent the impact of particle size.

**Table 1.** Description of the studied samples from BD section.

S.No.	Sample Name	Description
01	BD-01	Sandstone; thick to very thick bedded, light brown to red in color, fine to medium grained, moderate to highly compacted and cross-bedded.
02	BD-02	Sandstone; thick bedded massive, dark brown to red colored medium to coarse grained, compacted.
03	BD-03	Sandstone; thick to very thick bedded, reddish colored, fine to medium grained, moderately compacted and cross-bedded.
04	BD-05	Mudstone; thick to very thick bedded, reddish in appearance loose to moderately compacted.
05	BD-06	Sandstone; thick to very thick bedded massive, light red to dark red in color medium to coarse grained, compacted.
06	BD-07	Sandstone; thick bedded, massive, dark brown to reddish colored, fine to medium grained and compacted.
07	BD-08	Sandstone; thick to very thick bedded, light brown colored, medium to coarse grained, highly compacted and cross-bedded.
08	BD-09	Sandstone; thick bedded, light brown reddish colored, very fine to medium grained, highly compacted and cross-bedded.
09	BD-10	Sandstone; thick bedded, massive, dark brown in color, medium to coarse grained, highly compacted.

## 4. RESULTS:

### 4.1 Major Oxides

The whole rock geochemistry reported in present study is based on the investigations of nine (09) samples. The Table 2 presents the results of the major element geochemical investigation of the Pab Sandstone samples exposed at the BD section. Table 2 displays the ratios of the major oxides of BDS samples. The Pab Sandstone in studied section has high concentrations of silica, iron, and aluminum (66.43%, 6.58%, and 14.62%, on average) respectively, whereas all other oxides are found in lesser proportions. The  $\text{SiO}_2$

concentration of the Pab Sandstone at BD section is the dominantly prevalent major oxide in all the studied samples; ranging from 58.96% to 69.95% with an average of 66.43%. The Si/Al ratio in the Pab Sandstone sediments varies considerably. Since the  $\text{SiO}_2/\text{Al}_2\text{O}_3$  ratio rises with increasing quartz concentration at the expense of less resistant minerals during weathering, transportation, and recycling, it is employed as a maturity indicator for sandstones [22, 23]. Furthermore, low ratios of these variables refer to clay-rich shales and are utilized to determine mineralogical maturity; greater  $\text{SiO}_2/\text{Al}_2\text{O}_3$  ratios points to quartz-rich sandstone [24].

**Table 2.** Major element concentrations (wt.%) of selected samples of Pab Sandstone from BD section

Elements	BD-02	BD-03	BD-04	BD-05	BD-06	BD-07	BD-08	BD-09	BD-10
SiO <sub>2</sub>	65.10	69.95	68.32	58.96	68.92	68.38	67.11	67.95	63.21
TiO <sub>2</sub>	0.43	0.52	0.49	0.40	0.42	0.56	0.59	0.55	0.33
Al <sub>2</sub> O <sub>3</sub>	13.40	12.45	14.33	20.68	12.19	15.36	12.56	14.32	16.33
Fe <sub>2</sub> O <sub>3</sub>	13.64	5.65	5.13	11.26	6.82	3.96	4.98	5.65	2.13
MnO	0.88	0.78	0.81	0.56	0.78	0.88	0.84	0.78	0.71
MgO	0.37	0.86	0.85	0.36	0.78	0.35	0.65	0.86	0.74
CaO	2.19	3.78	4.68	2.36	3.48	3.89	6.23	4.12	11.12
Na <sub>2</sub> O	0.63	0.49	0.72	0.97	0.62	0.53	0.92	0.47	1.01
K <sub>2</sub> O	1.99	1.95	1.45	1.97	2.12	1.98	1.46	1.88	1.89
P <sub>2</sub> O <sub>5</sub>	0.29	0.45	0.49	0.47	0.43	0.29	0.19	0.45	0.65
LOI	0.84	3.45	2.72	1.99	3.45	3.10	3.99	3.45	2.45
Total	99.76	100.33	99.99	99.98	100.01	99.28	99.52	100.48	100.57

**Table 3.** Ratios of major elements of selected samples of Pab Sandstone from BD section.

Elements	BD-02	BD-03	BD-04	BD-05	BD-06	BD-07	BD-08	BD-09	BD-10
SiO <sub>2</sub> /Al <sub>2</sub> O <sub>3</sub>	4.86	5.62	4.77	2.85	5.65	4.45	5.34	4.75	3.87
Al <sub>2</sub> O <sub>3</sub> /SiO <sub>2</sub>	0.21	0.18	0.21	0.35	0.18	0.22	0.19	0.21	0.26
Al <sub>2</sub> O <sub>3</sub> /Na <sub>2</sub> O	21.27	25.41	19.90	21.32	19.66	28.98	13.65	30.47	16.17
K <sub>2</sub> O/Na <sub>2</sub> O	3.16	3.98	2.01	2.03	3.42	3.74	1.59	4.00	1.87
Na <sub>2</sub> O/K <sub>2</sub> O	0.32	0.25	0.50	0.49	0.29	0.27	0.63	0.25	0.53
Fe <sub>2</sub> O <sub>3</sub> /MgO	36.86	6.57	6.04	31.28	8.74	11.31	7.66	6.57	2.88
K <sub>2</sub> O/Al <sub>2</sub> O <sub>3</sub>	0.15	0.16	0.10	0.10	0.17	0.13	0.12	0.13	0.12
MnO/Fe <sub>2</sub> O <sub>3</sub>	0.06	0.14	0.16	0.05	0.11	0.22	0.17	0.14	0.33
MgO/Al <sub>2</sub> O <sub>3</sub>	0.03	0.07	0.06	0.02	0.06	0.02	0.05	0.06	0.05
TiO <sub>2</sub> /Al <sub>2</sub> O <sub>3</sub>	0.03	0.04	0.03	0.02	0.03	0.04	0.05	0.04	0.02
Fe <sub>2</sub> O <sub>3</sub> /Al <sub>2</sub> O <sub>3</sub>	1.02	0.45	0.36	0.54	0.56	0.26	0.40	0.39	0.13
Al <sub>2</sub> O <sub>3</sub> /TiO <sub>2</sub>	31.16	23.94	29.24	51.70	29.02	27.43	21.29	26.04	49.48
CIA	73.59	66.68	67.66	79.60	66.21	70.59	59.33	68.88	53.81
PIA	80.18	71.09	70.46	84.89	71.07	75.17	60.82	73.05	54.35

Significant concentration of alumina is present in the analyzed samples. The analyzed BD section samples have an average Al<sub>2</sub>O<sub>3</sub> content of 14.62 weight percent, with a range of 12.19 to 20.68%, which may be related to matrix and cement proportion. According to [25], compared to montmorillonite, kaolinite and illite have comparatively greater Al<sub>2</sub>O<sub>3</sub> contents. The ratio of Al<sub>2</sub>O<sub>3</sub>/Na<sub>2</sub>O, as suggested

by [26], is typically used to confirm the sediment maturity index. Higher Al<sub>2</sub>O<sub>3</sub>/Na<sub>2</sub>O ratios denote more mature sediments, whereas lower values will imply less mature sediments. The studied sediments had mild values of the aforementioned ratio, suggesting that they are less developed, most likely as a result of a shorter transport distance from the source location. According to [27], the K<sub>2</sub>O/Al<sub>2</sub>O<sub>3</sub> ratios indicate



the relative abundance of alkali compared to plagioclase feldspar. Alkali feldspar will predominate over other minerals if the  $K_2O/Al_2O_3$  ratio is more than 0.5. Conversely, if the aforementioned values are less than 0.4, they will suggest limited alkali feldspar, whereas values less than 0.3 suggest the existence of illite [27]. Table 3 summarizes the  $K_2O/Al_2O_3$  values of the studied samples. As shown by [28], the  $Al_2O_3/TiO_2$  ratio is another important and illuminating parameter for determining the composition of source rock. The bulk of the Pab sediments from BD section, appear to have originated from acidic igneous sources, based on the average  $Al_2O_3/TiO_2$  ratio of 32.14, and vary from 21.29 to 51.7. The iron oxide ( $Fe_2O_3$ ) concentration of the Pab Sandstone at BDS ranges from 2.13 % to 13.64%, with an average of 6.58 wt%.  $Fe_2O_3$ , which is often found in iron-bearing clays either as a coating on sand or on the clay particles themselves, is more abundant in sediments due to the extreme conditions of chemical weathering. Pab Sandstone at BD section has magnesium oxide (MgO) concentrations ranging from 0.35% to 0.86%, with an average of 0.65% in all samples. In all analyzed samples, the proportion of titanium oxide ( $TiO_2$ ) varies between 0.33% and 0.59%, with an average of 0.47%. It is generally considered that titanium is contributed to sedimentary rocks by a number of heavy minerals, such as rutile, ilmenite, and brookite.  $TiO_2/Al_2O_3$  ratios are particularly significant since they provide insight into the environmental conditions. According to [29] clays from humid climates have larger percentages of titanium and aluminum. It appears that the region underwent intense chemical weathering in a hot and humid climate during the Late Cretaceous period, as evidenced by the comparatively elevated concentration of titanium and higher percentage of aluminum

oxide in a few of the analyzed samples. In Pab Sandstone at BD section, the proportion of manganese oxide (MnO) varies from 0.56% to 0.88%, with an average of 0.78% in all 09 samples. The average calcium oxide (CaO) volume for the nine samples under study at BDS is 4.65%, with a range of 2.19 to 11.12%. Pab Sandstone has an average sodium oxide ( $Na_2O$ ) value of 0.70% across all samples, with a range of 0.47% to 1.01%. Pab Sandstone at BD section has an average potassium oxide ( $K_2O$ ) value of 1.85% over all 09 samples, ranging from 1.45% to 2.12 weight percent. The  $K_2O/Na_2O$  ratio was utilized by [23] to distinguish between the sandstone of Active Margin and Passive Continental Margin. According to [23] sandstones in active-margin settings have  $K_2O/Na_2O$  ratios smaller than 1, whereas those in passive-margin settings have ratios larger than 1. The average  $K_2O/Na_2O$  ratios at BD section are 2.86%, which indicate that the sediments under study belong to the passive margin. Phosphorous oxide ( $P_2O_5$ ), shows the presence of apatite, is present in the analyzed sediments at BD section and varies from 0.19 to 0.65%, with an average value of 0.41% in the studied samples.

## 4.2. Trace Elements

The trace element results of studied samples from the BD section are given in Table 4, whereas the Table 5 presents their ratios. The Zr content of the Pab Sandstone samples from the BD section ranges from 192 ppm to 322 ppm, with an average of 266 ppm. The average concentration of Th in examined samples is 7.69 ppm, with a range of 4.1 to 15.3 ppm. The La has an average of 26.25 ppm and ranges from 21 to 31 ppm. The average Hf value is 14.44 ppm, with values ranging from 10 ppm to 19 ppm.

In studied samples, the value of Ba varies from 78 to 291 with an average of 154.11 ppm. The average Sr concentration is 79.55 ppm, with a range of 44 to 108 ppm. The Sc ranges in value from 2.7 to 6.92 ppm, with an average of 4.99 ppm. With an average value of 5.35 ppm, the Co content varies from 2.3 to 9.3 ppm. The V has an average of 23.87 ppm and varies from as low as 11.9 to as high as 37 ppm. The average Ni value is 14.33 ppm, with a range of 6 to 31 ppm. The Cr vary from 13 to 50 ppm, with an average of 26.33 ppm. The U content ranges from 1 to 3 ppm, with an average of 1.44 ppm.

The ratios of these elements are helpful in determining the source of the sediments and the redox conditions that existed during the period of deposition. Many researchers, including [30, 31, 32] have claimed that trace elemental ratios, such as La/Sc, La/Co, Th/Sc, Cr/Th, and Th/Co, are very helpful in determining the provenance of sedimentary rocks.

The La/Sc concentration ratio in the Pab Sandstone samples at BD section range from 3.03 ppm to 10.74 ppm, with an average of 5.74 ppm. The average Th/Sc ratio is 1.82 ppm, with a range of 1.1 to 3.36 ppm. La/Co ratios range from 3.01 to 11.87 ppm, with an average of 5.88 ppm. The Cr/Th ratios vary from 1.43 to 12.2 ppm with an average of 3.67

ppm at BDS, while Th/Co ratios range from 0.71 to 3.96 ppm with an average of 1.94 ppm. These data unequivocally show that the bulk of the sediments that comprise the Pab Sandstone originated from an acidic source, with a little contribution from basic igneous rocks. The bulk of the examined Pab Sandstone samples at BD section had Cr/Th ratios above 2.5, average 3.67 ppm, further confirming that felsic/granitoid rock is the primary source of the sediments under study. A small number of samples had Cr/Th ratios below 2 ppm. The Indian shield exposures containing felsic/granitoid rocks are still present in the southeast of the study region. These rocks are primarily granitic with a few simple intrusions in the form of diorite or dolerite dikes with varying compositions [33, 34, 35, 36, 37, 38]. It is believed that sediments of Pab Sandstone were taken from the Indian shield based on the trace element concentrations and ratios. The BD section samples have average Ba content of 154.1 ppm, with the concentration ranging from 78 ppm to 291 ppm. The average Sr content in the sediments under study is 79.5 ppm, with a range of 44 to 108 ppm. Higher Sr levels together with Ba are typically found in felsic igneous rocks, such as granite, as stated by [39].

**Table 4.** Trace element concentrations (in ppm) of studied samples from BD section.

Element	BD-01	BD-02	BD-03	BD-05	BD-06	BD-07	BD-08	BD-09	BD-10
Sc	4.55	4.95	6.81	6.92	5	2.7	6.1	3.8	4.12
V	33	29	21	11.9	23	37	14	21	25
Cr	31	15	26	29	31	50	28	14	13
Ni	17	16	31	15	9	11	13	6	11

Cu	12	8	10	7	18	9	11	8	13
Zn	36	83	63	98	22	9	18	14	23
As	1	1.3	1.1	1	2	2.16	1.25	2.32	2
Rb	3	9	5	8.1	2.8	6	2	5	6
Sr	108	79	77	78	103	103	66	44	58
Hf	13	16	15	11	18	13	10	15	19
Zr	208	192	299	260	284	278	271	286	322
Nb	13	10	23	8	27	30	21	26	24
Mo	3.5	4	2.3	2.61	1.5	2	1.1	1.14	3.2
Ba	269	291	78	94	178	188	110	88	91
La	22	25	28	21	27	29	31	26	27.3
Ce	43	56	62	48	92	102	43	56	91
Pb	12	14	9	11	6	8	12	7	5
Th	15.3	9.1	7.52	7.85	8.51	4.1	8.85	7.8	9.1
Co	6.75	3.5	9.3	3.6	7	5.8	3.45	6.5	2.3
U	2	1	1	3	1	1	1	2	1

**Table 5.** Ratios of trace elements of studied samples from BD section.

Elements	BD-01	BD-02	BD-03	BD-05	BD-06	BD-07	BD-08	BD-09	BD-10
La/Co	3.26	7.14	3.01	5.83	3.86	5.00	8.99	4.00	11.87
Th/Co	2.27	2.60	0.81	2.18	1.22	0.71	2.57	1.20	3.96
La/Sc	4.84	5.05	4.11	3.03	5.40	10.74	5.08	6.84	6.63
Th/Sc	3.36	1.84	1.10	1.13	1.70	1.52	1.51	2.05	2.21
Th/Cr	0.49	0.61	0.29	0.27	0.27	0.08	0.40	0.56	0.70
Rb/Sr	0.03	0.11	0.06	0.10	0.03	0.06	0.03	0.11	0.10
Sr/Hf	8.31	4.94	5.13	7.09	5.72	7.92	6.60	2.93	3.05
Th/U	7.65	9.10	7.52	2.62	8.51	4.10	8.85	3.90	9.10
U/Th	0.13	0.11	0.13	0.38	0.12	0.24	0.11	0.26	0.11
Ni/Co	2.52	4.57	3.33	4.17	1.29	1.90	3.77	0.92	4.78
Cu/Zn	0.33	0.10	0.16	0.07	0.82	1.00	0.61	0.57	0.57
V/Cr	1.06	1.93	0.81	0.41	0.74	0.74	0.50	1.50	1.92
Sr/Ba	0.40	0.27	0.99	0.83	0.58	0.55	0.60	0.50	0.64
Ba/Sr	2.49	3.68	1.01	1.21	1.73	1.83	1.67	2.00	1.57
Zr/Sc	45.71	38.79	43.91	37.57	56.80	102.96	44.43	75.26	78.16
Cr/Zr	0.15	0.08	0.09	0.11	0.11	0.18	0.10	0.05	0.04
Sc/Th	0.30	0.54	0.91	0.88	0.59	0.66	0.69	0.49	0.45
La/Th	1.44	2.75	3.72	2.68	3.17	7.07	3.50	3.33	3.00
La/Co	3.26	7.14	3.01	5.83	3.86	5.00	8.99	4.00	11.87
Ba/Sc	59.12	58.79	11.45	13.58	35.60	69.63	18.03	23.16	22.09
Ba/Co	39.85	83.14	8.39	26.11	25.43	32.41	31.88	13.54	39.57
Cr/Th	2.03	1.65	3.46	3.69	3.64	12.20	3.16	1.79	1.43
Sc/Th	0.30	0.54	0.91	0.88	0.59	0.66	0.69	0.49	0.45

## 5. DISCUSSION

Higher SiO<sub>2</sub> concentrations are found in the investigated sediments as a result of the general abundance of quartz, though all the silica is not always the part of crystal structure

of quartz but some of the silica is also accommodated within the clays along with certain other silicate minerals. Al<sub>2</sub>O<sub>3</sub>, which ranges from 12.19 weight percent to 20.68



weight percent, is the second most common oxide in the studied sandstone and can be related to the occurrence of certain clay minerals. [15, 11] reported low amount of feldspar in Pab Sandstone and suggested the potential alteration of feldspar into certain clay minerals. The overall abundance of  $\text{Al}_2\text{O}_3$  in studied sediments may possibly be related with the alteration of feldspar.  $\text{Fe}_2\text{O}_3$  and  $\text{CaO}$  range from 2.13 to 13.64 weight percent and 2.19 to 11.12 weight percent respectively in the sediments of Pab Sandstone; greater  $\text{Fe}_2\text{O}_3$  is associated with iron oxide cement, while  $\text{CaO}$  is representative of calcite cement. As per [45] there exists a correlation between the  $\text{K}_2\text{O}$  content and the orthoclase feldspar and mica content, whereas the plagioclase feldspar and  $\text{Na}_2\text{O}$  content are linked. The investigated sediments exhibit deficiencies in  $\text{K}_2\text{O}$  and  $\text{Na}_2\text{O}$ , which aligns with the petrographic observations of Pab Sandstone sediments as reported by [11].

The existence of potassium feldspar, muscovite, biotite, and illite is suggested by the increased  $\text{K}_2\text{O}$  relative to  $\text{Na}_2\text{O}$  values, according to [46]. Major oxides including  $\text{SiO}_2$ ,  $\text{CaO}$ ,  $\text{MgO}$ ,  $\text{Na}_2\text{O}$ , and  $\text{K}_2\text{O}$  were measured and plotted on a ternary diagram proposed by [31] in order to determine the provenance of the Pab Sandstone. Most of the samples in this diagram are dispersed near granitic sources, but some are plotted in between basaltic and granitic fields; this could be because of the minor contributions from the mafic sources. In the southeast of the research area, the Indian shield rocks contain

minor intrusions in the form of diorite and dolerite dikes of various compositions and reported by many authors (e.g., [33, 34, 35, 36, 37, 38]).

Geochemical parameters including  $\text{TiO}_2$  and Zr were used by [28] to distinguish acidic, intermediate and mafic source; the studied sediments were plotted in this model and depict strong affinity with the acidic rocks; though few samples were plotted close to intermediate fields suggesting slight input from basic sources.

The trace elements like La, Sc, Th, Co, and the ratios of La/Sc and Th/Co, were used to identify the source, whether it was felsic or basic. Employing the La/Sc and Th/Co ratios from the [40] scheme, it is evident that the BD section samples (Fig. 4) fall into the acid rocks field. Based on the La/Sc and Th/Co model suggested by [40] it is possible that granitic rocks contributed sediments to the Pab Sandstone. According to [39] felsic igneous rocks, including granite, typically have elevated levels of Sr and Ba. The studied sediment have higher Sr and Ba values suggesting granitic source for the Pab Sandstone sediments at BD section. Based on the current whole rock geochemical data along with some previous studies (e.g., [12, 47, 16, 11]), it is established that Pab Sandstone sediments were extracted from the granitic rocks of the Indian shield which are exposed in the southeast of the research area in Pakistan (Nagar Parkar Igneous Complex) as well as in India (Malani Igneous Suite). On the basis of PIA and CIA values; moderate to

extreme weathering conditions in the source region are concluded for studied sediments of the Pab Sandstone.

### 5.1 Provenance and Tectonics

To determine the provenance type, the major oxide parameters such as  $\text{SiO}_2$ ,  $\text{CaO}$ ,  $\text{MgO}$ ,  $\text{Na}_2\text{O}$ , and  $\text{K}_2\text{O}$ , as well as their relationships are crucial. Consequently, they are employed in the current study to examine the provenance of Pab sediments; and is accomplished by applying the  $\text{Si}/10 - (\text{Ca} + \text{Mg}) - (\text{Na} + \text{K})$  ternary plot-based categorization approach that was suggested by [31]. The major oxide values when plotted on ternary

model the majority of the samples are dispersed close to granitic field; this type of plotting may be explained by the relatively high proportion of  $\text{SiO}_2$  found in the sediments under study (Fig. 2). Consequently, confirming the granitic provenance of Pab sediments as opposed to mafic, ultramafic, or metamorphic sources. The source of the Pab sediments is thus thought to be the granitic rocks of Indian Shield, as indicated by the geochemical data.

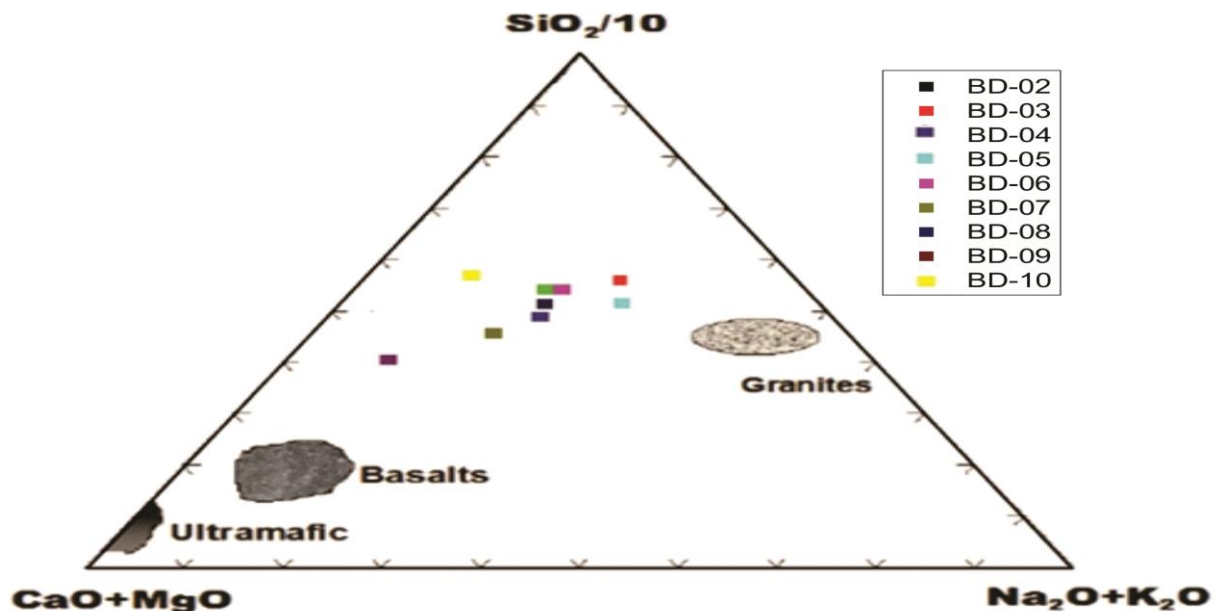


**Fig. 2.**  $\text{Na}_2\text{O} + \text{K}_2\text{O}$ ,  $\text{SiO}_2/10 - \text{CaO} + \text{MgO}$  ternary diagram of Pab sediments at BD section to illustrate possible affinities with acidic, basic or ultrabasic rocks (after [31]).

[28] distinguished the main igneous rock types, such as the mafic, intermediate, and felsic, using the concentrations of  $\text{TiO}_2$  and Zr. The Pab Sandstone sediments from the BD section primarily plot in the field of acidic rocks according to this  $\text{TiO}_2$  against Zr model, with only a small number of samples falling into the

category of intermediate rocks (Fig. 3). In the southeast of the research area acidic igneous rocks like granites, microgranites, aplites and rhyolites are exposed which may have contributed sediments for the Pab Sandstone. However, the mixing of many sources may be the reason for the scattering of a few samples

around intermediate fields. A small number of mafic dikes are also seen in the Indian shield

rocks, which may have provided some sediments for the Pab Sandstone together with the granitoids.

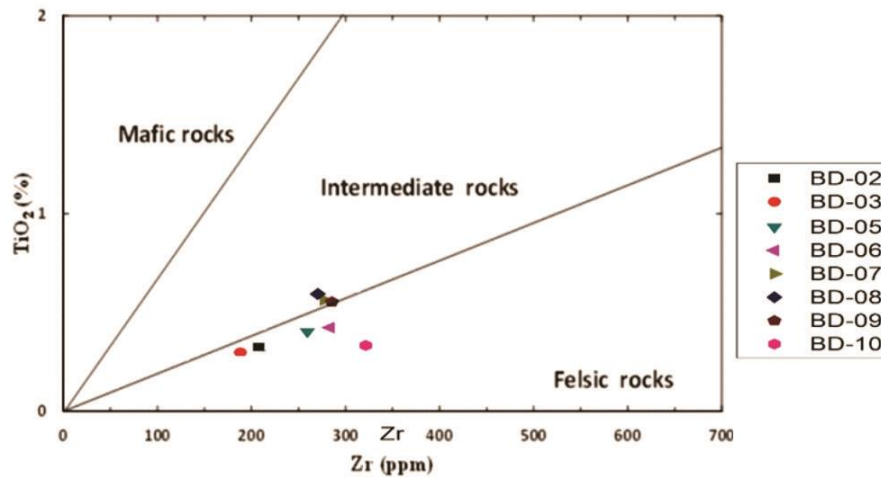


Fig. 3. TiO<sub>2</sub> versus Zr diagram of Pab Sandstone at BD section (fields after [28]).

Identification of the source, whether basic or felsic, was done using trace elements such as La, Sc, Th, and Co, as well as ratios of La/Sc and Th/Co. Using the La/Sc and Th/Co ratios in the [40] scheme, the samples of BD section

(Fig. 4) clearly plot within the field of acid rocks. The [40] La/Sc and Th/Co model suggests that like the [28] model as described above; the granitoid rocks of the Indian Shield have contributed sediments for the Pab Sandstone.

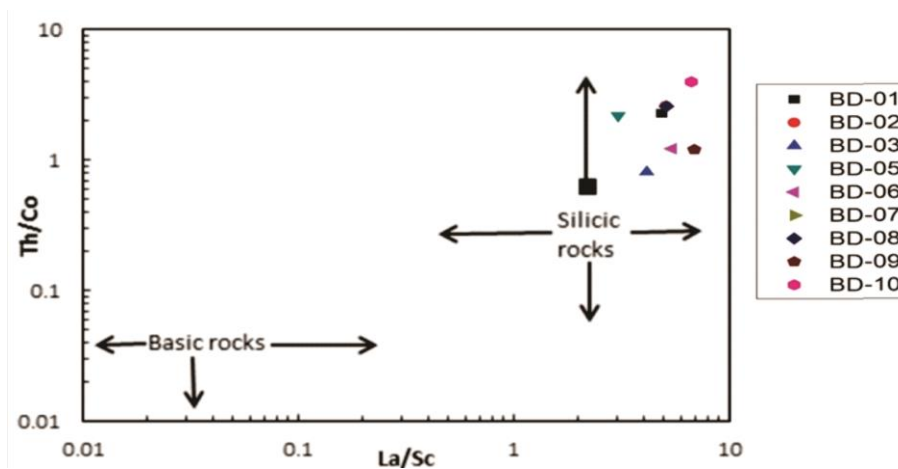


Fig. 4. Th/Co versus La/Sc diagram of Pab Sandstone at BD section (Fields after [40]).

## 5.2 Paleoweathering

Prior to mobility or transportation, the weathering conditions at the source region should be examined as the main oxides concentration might be impacted by

diagenetic processes [41, 48, 49]. The tectonics that exposes the source rocks and provides information on the relief, along with the composition of the source rock and climatic conditions are the key factors

governing the weathering conditions of the source region [42]. Alkali and alkaline earth elements can be used to assess the weathering history of sediments [43]. According to [42] weathering results in the decrease of alkali and alkaline earth elements.

To evaluate the paleoweathering trend, the Chemical Index of Alteration (CIA) and Plagioclase Index of Alteration (PIA) have been used for last few decades. The chemical weathering impact is minimal when the CIA value is less than 50, and it is highly significant when the CIA value is greater than 75. According to Table 2, the CIA values of the studied sediments range from 53.81 to 79.6, indicating a moderate to intense weathering conditions. [44] proposed the Plagioclase Index of Alteration (PIA), which measures the oxides including  $\text{Al}_2\text{O}_3$ ,  $\text{CaO}$ ,  $\text{K}_2\text{O}$ , and  $\text{Na}_2\text{O}$ . According to [44] a PIA value of 50 indicates comparatively undisturbed rocks, whereas values up to 100 indicate severe weathering. According to Table 2, the PIA values of the investigated sediments range from 54.35 to 84.89, indicating moderate to high weathering conditions at the source.

## CONCLUSIONS

Based on geochemical investigations of Late Cretaceous Pab Sandstone exposed in the Laki Range, the most common oxide found is silica, which is followed by aluminum oxide, calcium oxide, iron oxide respectively; all other oxides are present in lesser amount. In addition to major oxides trace elements such as Th, Zr, Ba, Sr and La are observed in

abundance in contrast to Sc, Co, V, Cr and Ni. The major oxide and trace element data along with different discrimination diagrams suggest the felsic/granitic source dominantly in comparison to mafic and ultramafic rocks. The results of major oxide analyses are consistent with the trace element geochemistry findings. The CIA and PIA values indicate that the examined sediments experienced moderate to intense weathering conditions. The vast landmass of the Indian Shield (Craton) is the source of the Pab Sandstone sediments.

## DECLARATIONS

**Conflicts of interest** Authors have none to declare

**Data availability:** Not applicable

**Code availability:** Not applicable

## REFERENCES

- [1] E.W. Vredenburg, The Cretaceous Orbitoides of India. Indian Geological Survey Memoirs, 36, (1908) 171–213.
- [2] M.D. Williams, Stratigraphy of the Lower Indus Basin, West Pakistan. In 5th World Petroleum Congress (1959).
- [3] HSC, Reconnaissance geology of part of West Pakistan: Colombo Plan Co-operative Project, published for the Government of Pakistan by the Government of Canada. Toronto, Canada (1960).
- [4] P.C. Van de Kamp, B.E. Leake, Petrology and geochemistry of siliciclastic rocks of mixed feldspathic and ophiolitic provenance in the Northern Apennines, Italy. *Chemical Geology*, 122(1-4), (1995) 1-20.
- [5] A.M. Cingolani, M.R. Cabido, D. Renison, V. Solís Neffa, Combined effects of environment and grazing on vegetation structure in Argentine

- granite grasslands. *Journal of Vegetation Science*, 14(2), (2003) 223-232.
- [6] J.S. Armstrong-Altrin, S.P. Verma, Critical evaluation of six tectonic setting discrimination diagrams using geochemical data of Neogene sediments from known tectonic settings. *Sedimentary Geology*, 177(1-2), (2005) 115-129.
- [7] R. Nagarajan, J. Madhavaraju, R. Nagendra, J.S. Armstrong-Altrin, J. Moutte, Geochemistry of Neoproterozoic shales of the Rabanpalli Formation, Bhima Basin, Northern Karnataka, southern India: Implications for provenance and paleoredox conditions. *Revista Mexicana de Ciencias Geológicas* 24, (2007) 150-160.
- [8] M. Jafarzadeh, M. Hosseini-Barzi, Petrography and geochemistry of Ahwaz Sandstone Member of Asmari Formation, Zagros, Iran: implications on provenance and tectonic setting. *Revistamexicana de cienciasgeológicas*, 25(2), (2008) 247-260.
- [9] S. Pandey, S.K. Parcha, Provenance, tectonic setting and source area weathering of the lower Cambrian sediments of the Parahio valley in the Spiti basin, India. *Journal of Earth System Science*, 126, (2017) 1-16.
- [10] Q.D. Khokhar, Provenance and Tectonic Setting of Bara Formation, Southern Indus Basin, Pakistan. Doctoral thesis, University of Sindh, Jamshoro (2019).
- [11] G.M. Thebo, S.H. Solangi, M.H. Agheem, M.A. Solangi, A.H. Markhand, K.A. Memon, Petrography and Geochemistry of late Cretaceous Pab Sandstone, Laki range, Southern Indus Basin, Pakistan: implications for Provenance and Paleoclimate. *Journal of Himalayan Earth Science*, 56(1) (2023).
- [12] A.M. Kassi, A.R. Qureshi, M.A. Farooqui, D.M. Kakar, Petrology and grain size characters of the Pab Sandstone of part of the Loralai and Khuzdar Districts. *Geological Bulletin University of Peshawar*, 24, (1991) 99-108.
- [13] M. Sultan, M. Jr. Gipson, Reservoir potential of the Maastrichtian Pab Sandstone in the eastern Sulaiman Fold-Belt. *Pakistan Journal of Petroleum Geology* 18, (1995) 309–328.
- [14] A.S. Khan, G. Kelling, M. Umar, A.M. Kassi, Depositional environments and reservoir assessment of Late Cretaceous sandstones in the south central Kirthar foldbelt. *Pak J Petrol Geol* 25 (2002) 373–406.
- [15] M. Umar, Facies Distribution, Depositional Environment, Provenance and Reservoir Characters of Upper Cretaceous Succession, Kirthar Fold Belt Pakistan. Ph.D. Thesis, Centre of Excellence in Mineralogy, University of Balochistan, Pakistan, (2007) p. 191.
- [16] M. Umar, H. Friis, A.S. Khan, A.M. Kassi, A.K. Kasi, The effects of diagenesis on the reservoir characters in sandstones of the Late Cretaceous Pab Formation, Kirthar Fold Belt, southern Pakistan. *J Asian Earth Sci* 40 (2011) 622–635.
- [17] D.D. Schelling, Frontal structural geometries and detachment tectonics of the northeastern Karachi arc, Southern Kirthar Range, Pakistan. *Special Paper-Geological Society of America*, 328 (1999) 287–302.
- [18] M.H. Agheem, S.H. Solangi, A.A. Hakro, A.S. Mastoi, I. Siddiqui, Major element geochemistry of basalt exposed at Ranikot area, lower Indus basin, Pakistan. *Journal of Himalayan Earth Sciences*, 44(2), (2011) 33–43.
- [19] M.H. Agheem, M.Q. Jan, S.H. Solangi, A. Laghari, H. Dars, Basaltic flows in the Laki Range of the Lower Indus Basin, Sindh, Pakistan: Evidence for northwestern extension of the Deccan traps, First International Workshop on Tethyan Orogenesis and Metallogeny in Asia and Cooperation among Institutions of Higher Education, China University of Geosciences, Wuhan, China (2014).
- [20] R. Tertian, F. Claisse, Principles of quantitative X-ray fluorescence analysis. Heyden (1982).

- [21] K. Norrish, B.W. Chappell, X-ray fluorescence spectrometry. In "Physical Methods in Determinative Mineralogy".(Ed. J. Zussman.). Academic Press: London (1977).
- [22] B.P. Roser, R.J. Korsch, Determination of tectonic setting of sandstone-mudstone suites using SiO<sub>2</sub> content and K<sub>2</sub>O/Na<sub>2</sub>O ratio. *The Journal of Geology*, 94(5), (1986) 635–650.
- [23] J.B. Maynard, R. Valloni, H.S. Yu, Composition of modern deep sea sands from arc-related basins. In: Legget, J.K., (Ed.), *Trench-Forearc Geology: Sedimentation and Tectonics on Modern and Ancient Active Plate Margins*. Geol. Soc. Lond. Spec. Pub. 10, (1982) 551-561.
- [24] F.J. Pettijohn, P.E. Potter, R. Siever, Production and provenance of sand. In *Sand and Sandstone* (pp. 294-326). Springer, New York, NY (1972).
- [25] C.E. Weaver, L.B. Pollard, *The chemistry clay minerals*. New York, USA.: Elsevier (1973).
- [26] F.J. Pettijohn, *Sedimentary Rocks* (2nd ed.). New York, USA.: Harper and Brothers (1957).
- [27] R. Cox, D.R. Lowe, R.L. Cullers, The influence of sediment recycling and basement composition on evolution of mudrock chemistry in the southwestern United States. *Geochim. Cosmochim. Acta* 59, (1995) 2919-2940.
- [28] K.I. Hayashi, H. Fujisawa, H.D. Holland, H. Ohmoto, Geochemistry of ~1.9 Ga sedimentary rocks from northeastern Labrador, Canada. *Geochimica et Cosmochimica Acta*, 61(19), (1997) 4115–4137.
- [29] A.A. Migdisov, On the titanium/aluminium ratio in sedimentary rocks. *Geochimica*, 2, (1960) 149-163.
- [30] K.C. Condie, D.J. Wronkiewicz, The Cr/Th ratio in Precambrian pelites from the Kaapvaal craton as an index of craton evolution. *Earth and Planetary Science Letters* 97, (1990) 256-267.
- [31] S.R. Taylor, S.M. McLennan, *The Continental Crust: Its Composition and Evolution*. Blackwell Scientific Publications, Oxford (1985) 312pp.
- [32] R.L. Cullers, S. Chaudhuri, N. Kilbane, R. Koch, Rare earths in size fractions and sedimentary rocks of Pennsylvanian-Permian age from the mid-continent of the U.S.A. *Geochim. Cosmochim. Acta*. 43, (1979) 1285-1302.
- [33] M.Q. Jan, A. Laghari, M.H. Agheem, S. Anjum, Geology and Petrography of the Nagar Parkar igneous complex, southeastern Sindh: the Dinsi body. *Jr. Himalayan Earth Sci. Univ. Peshawar*, 47(2), (2014) 1-14.
- [34] M.Q. Jan, M.H. Agheem, A. Laghari, S. Anjum, Geology and Petrography of the Nagar Parkar igneous complex, southeastern Sindh: the Wadhrai body. *Jr. Himalayan Earth Sci., Univ. Peshawar*, 49(1), (2016) 17-29.
- [35] M.Q. Jan, M.H. Agheem, A. Laghari, S. Anjum, Geology and petrography of the Nagar Parkar igneous complex, southeastern Sindh, Pakistan: the Kharsar body; *Jr. Geol. Soc. India*, 89, (2017) 91-98.
- [36] M.Q. Jan, M.H. Agheem, T. Khan, H.U. Rehman, A.H. Markhand, Geochemistry and Petrogenesis of the Wadhrai Granite Stock of the Malani Igneous Suite in Nagar Parkar Area, SE Pakistan. *Minerals*, 12, 1240 (2022).
- [37] A. Laghari, M.Q. Jan, A. Khan, M.H. Agheem, A.G. Sahito, S. Anjum, Petrography and major element chemistry of mafic dykes in the Nagar Parkar Igneous Complex, Tharparkar, Sindh. *Journal of Himalayan Earth Sciences* 46(1) (2013) 1-11.
- [38] A.H. Markhand, Q.K. Xia, M.H. Agheem, L. Jia, U-Pb zircon dating and geochemistry of the rocks at Wadhrai body, Nagar Parkar Igneous Complex, Sindh, Pakistan. *Sindh Univ. Res. Jour. (Sci. Ser.)* Vol.49 (1) (2017) 01-06.
- [39] A.K. Krishna, K. R. Mohan, N.N. Murthy, A multivariate statistical approach for monitoring



- of heavy metals in sediments: a case study from Wailpalli Watershed, Nalgonda District, Andhra Pradesh, India. *Res J Environ Earth Sci*, 3(2), (2011) 103-113.
- [40] R.L. Cullers, Implications of elemental concentrations for provenance, redox conditions, and metamorphic studies of shales and limestones near Pueblo, CO, USA. *Chem. Geol.* 191, (2002) 305-327.
- [41] S.M. McLennan, Relationships between the trace element composition of sedimentary rocks and upper continental crust. *Geochemistry Geophysics Geosystems* 2, (2001).
- [42] B.P. Roser, R.J. Korsch, Provenance signatures of sandstone mudstone suites determined using discriminant function analysis of major element data. *Chemical Geology*, 67, (1988) 119–139.
- [43] H.W. Nesbitt, G.M. Young, Formation and diagenesis of weathering profile. *J. Geol.* 97, (1989) 129-147.
- [44] C.M. Fedo, H.W. Nesbitt, G.M. Young, Unraveling the effects of potassium metasomatism in sedimentary rocks and paleosols, with implications for paleoweathering conditions and provenance. *Geology* 23, (1995) 921-924.
- [45] M. Khanehbad, R. Moussavi-Harami, A. Mahboubi, M. Nadjafi, M.H. Mahmudy-Gharaie, Geochemistry of Carboniferous sandstones (Sardar Formation), East-Central Iran: implication for provenance and tectonic setting. *Acta Geologica Sinica*, vol.86, issue 5 (2012) pp. 1200-1210.
- [46] S. Osae, D.K. Asiedu, B. Banoeng-Yakubo, C. Koeberl, S.B. Dampare, Provenance and tectonic setting of Late Proterozoic Buem sandstones of southeastern Ghana: Evidence from geochemistry and detrital modes. *J. African Earth Sciences* 44, (2006) 85-96.
- [47] M.A. Kakar, S. Ghazi, A.S. Khan, A.M. Kasi, Tanzila hanif, Petrology and provenance of the upper cretaceous mughalkot formation and pab sandstone, western Sulaiman thrust and fold belt, Pakistan. *Geol. Bull. Punjab Univ*, 45, (2010) 1-23.
- [48] H. Zhang, L. Qiu, D.P. Yan, Z. Zhao, K. Cai, J. Zhang, S. Chen, Y. Li, Y. Song, Y. Zheng, S. Sun, F. Gong, S. Ariser, Late-Permian subduction-to-collision transition and closure of Paleo-Asian Ocean in eastern Central Asian Orogenic Belt: Evidence from borehole cores in the Songliao Basin, Northeast China. *Gondwana Research*, Volume 122, (2023) pp. 74-92.
- [49] L. Qiu, D.P. Yan, W.X. Yang, J. Wang, X. Tang, S. Ariser. Early to Middle Triassic sedimentary records in the Youjiang Basin, South China: Implications for Indosinian orogenesis. *Journal of Asian Earth Sciences*, Volume 141, Part A, (2017), pp 125-139.

Received: 16 February 2024. Revised/Accepted: 30 March 2024.



This work is licensed under a [Creative Commons Attribution 4.0 International License](https://creativecommons.org/licenses/by/4.0/).

---